

Multiphoton Ionization/Dissociation of $\text{Ge}(\text{CH}_3)_4$ and $\text{Ge}(\text{C}_2\text{H}_5)_4$

Jeunghee Park,* Yoo Nam Kang, Nam Ung Song,[†] and Dongho Kim[‡]

Department of Chemistry, Korea University, 208 Seochangdong Chochiwon, Chungnam 339-700, Korea

[†]Spectroscopy Laboratory, Korean Research Institute of Standards and Science, Taedok Science Town,

Taejon 305-500, Korea

Received December 7, 1998

Laser-assisted metal organic chemical vapor deposition (LCVD) was proved to be an efficient technique for the deposition of a large variety of thin films.¹ The CVD precursor can produce metal atoms directly in the gas phase, or deposits in a partially fragmented form before undergoing further fragmentation. Therefore, the understanding of the photofragmentation process could lead to improved film properties and growth rate, and a redesign of the CVD precursor which could yield higher purity films.

Ge is one of the most widely used semiconductor materials, often doped with other elements, and employed as a transistor element in electronic applications. Osmundsen *et al.* investigated the growth of Ge thin film by photodissociating GeH_4 at 248 nm.² Fajgar *et al.* investigated CO_2 laser SF_6 -photosensitized decomposition of ethoxy(trimethyl)germanium (ETG) and tetramethylgermanium (TMG), assessing the potential for Ge CVD film precursor.³ Stanely also reported a CO_2 laser SF_6 -photosensitized depletion rate of TMG.⁴ For the gas phase dissociation, Antman *et al.* reported the non-mass selected REMPI (resonance enhanced multiphoton ionization) spectrum of Ge neutral atom and TOF (Time-of-Flight) mass spectrum of fragment ions from the photodissociation of $\text{Ge}(\text{C}_2\text{H}_5)_4$ (TEG) at 355 nm. They suggested a possible dissociation mechanism for the formation of Ge atom.⁵

This paper elucidates the photoionization and fragmentation mechanism of two Ge CVD precursors, $\text{Ge}(\text{CH}_3)_4$ (TMG) and $\text{Ge}(\text{C}_2\text{H}_5)_4$ (TEG), in gas phase at 355 nm and 266 nm. The MPI/TOF mass spectra of the two precursors were measured and compared.

The TOF mass spectrometer (R. M. Jordan Company) consists of two chambers, a source chamber and a TOF chamber, differentially pumped by a pair of liquid-nitrogen baffled oil diffusion pumps. The pressure in the source chamber, which was measured by an ion gauge, was always less than 10^{-5} Torr. The TOF chamber was evacuated by a turbo molecular pump. The flight length was 1 m, with the pressure maintained in the range of 10^{-7} Torr. The mass resolution was measured to be 0.34 amu for mass 128 amu. The diluted sample (1/50 for TEG and 1/10 for TMG) was admitted by the He gas to the source region via a 0.2 mm-diameter pulsed nozzle valve. The backing pressure of the He gas was 1–2 atm. Ions were detected by a MCP (microchannel plate), the ion arrival time spectrum was sent directly to a digital oscilloscope (Hewlett Packard 54503A) and averaged for 1000 laser pulses. The averaged ion arrival time spectrum was converted to the mass spectrum by calibration using a

mixture of I_2 and He gas. The laser beam from a Nd-YAG laser (Spectron), whose output diameter was adjusted to 4 mm by using an iris, was focused into the molecular beam with a 60-cm focal length lens. The laser intensity, monitored using a surface calorimeter (Laser Focus Precision Corp.) positioned at the exit window, was increased up to 8 mJ/pulse at 266 nm and 40 mJ/pulse at 355 nm. TEG (Aldrich, 98%) and TMG (Aldrich, 98%) was degassed by several freeze (77 K)-pump-thaw cycles, then used without further purification.

Figure 1(A) shows the MPI/TOF mass spectrum of TEG at 355 nm 8 mJ/pulse for only the Ge ion. The molecular beam of TEG/He was irradiated by the focused laser beam, with the lens positioned at the focal distance (60 cm). The pulse width of the nozzle was 250 s. The 5 peaks correspond to 5 isotopes of natural Ge: ^{70}Ge , ^{72}Ge , ^{73}Ge , ^{74}Ge , and ^{76}Ge . Their abundance in percentage are 21.23% (^{70}Ge), 27.66% (^{72}Ge), 7.73% (^{73}Ge), 35.94% (^{74}Ge), and 7.44% (^{76}Ge). The log-log plot of the Ge ion signal vs. the laser intensity (2–40 mJ/pulse) is shown in the inset of Figure 1(A). The linear fit

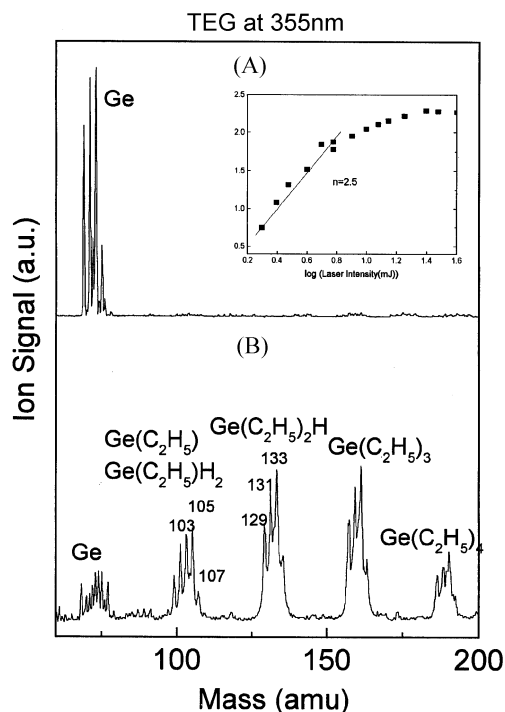


Figure 1. The MPI (355 nm)/TOF mass spectrum of TEG at (A) 2.1 kJ/cm^2 and (B) 2.3 J/cm^2 per pulse (see the text). The inset of (A) shows the log-log plot of the Ge ion signal vs. the laser intensity (mJ/pulse), whose slope is 2.5 ± 0.1 .

for the data points at the laser intensity range of 2-6 mJ/pulse yields the slope as 2.5 ± 0.1 . Figure 1(B) shows the TOF mass spectrum of TEG when the laser beam is defocused by moving the lens from the focal position by 10 cm. The pulse width of the nozzle is increased to 800 μs in order to obtain enough S/N ratio. Assuming that the laser beam profile is a Gaussian function, the focused spot size (radius) of the 60-cm focal lens is estimated as 11 μm . When the lens is moved 10 cm for loose focusing, the laser beam radius at the molecular beam increases to about 330 μm , and the laser intensity decreases by a factor of 900. Thus, the laser intensities per unit area (cm^2) at the molecular beam are 2.1 $\text{kJ}/\text{cm}^2 \cdot \text{pulse}$ for Figure 1(A) and 2.3 $\text{J}/\text{cm}^2 \cdot \text{pulse}$ for Figure 1(B). At 2.3 $\text{J}/\text{cm}^2 \cdot \text{pulse}$, all alkyl germanium ions such as mono-, di-, and tri-ethyl germanium ions as well as the parent ion are observed.

Figure 1(B) shows the peaks at mass 129, 131, and 133, which correspond to the $\text{Ge}(\text{C}_2\text{H}_5)_2\text{H}^+$ ion of ^{70}Ge , ^{72}Ge , and ^{74}Ge , respectively. Interestingly, the $\text{Ge}(\text{C}_2\text{H}_5)_2^+$ ion peaks are not observed. The strong peak at 105 can be attributed to the $^{74}\text{Ge}(\text{C}_2\text{H}_5)_2\text{H}^+$ ion and the weak peak at 107 can be attributed to the $^{76}\text{Ge}(\text{C}_2\text{H}_5)_2\text{H}^+$ ion. The Ge ions consist of the mass 70-77, indicating the existence of Ge hydride ions.

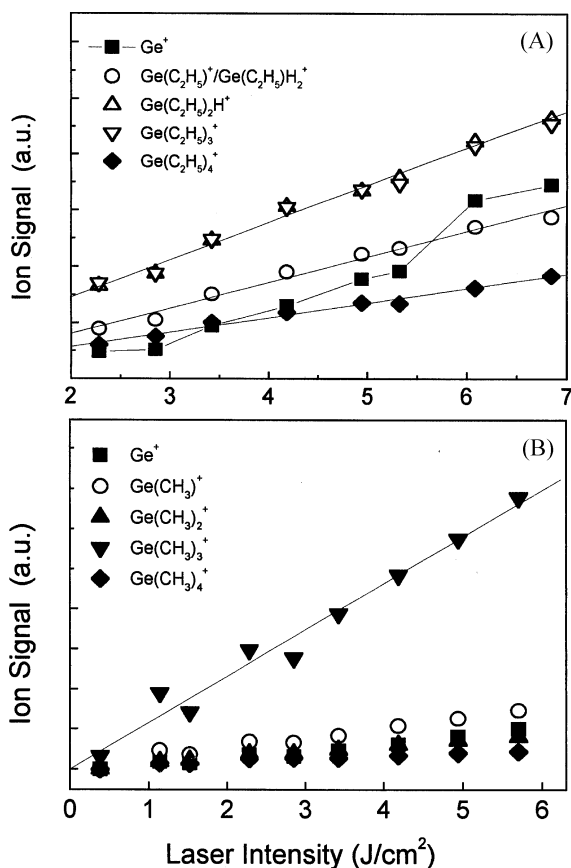


Figure 2. The ion signal vs. the laser intensity (J/cm^2 per pulse) for (A) TEG and (B) TMG at 355 nm. (A) The data points of parent, $\text{Ge}(\text{C}_2\text{H}_5)_3^+$, $\text{Ge}(\text{C}_2\text{H}_5)_2\text{H}^+$, and $\text{Ge}(\text{C}_2\text{H}_5)^+$ ions are fitted by a line. The data points of the Ge^+ ion is connected by the line to show a nonlinear dependence. (B) The ion signal of $\text{Ge}(\text{CH}_3)_3^+$ ion grows linearly with the laser intensity, as fitted by a line.

The ethyl germanium ion signals as a function of laser intensity in $\text{J}/\text{cm}^2 \cdot \text{pulse}$ are plotted in Figure 2(A), displaying a linear dependence. The $\text{Ge}(\text{C}_2\text{H}_5)_3^+$ and $\text{Ge}(\text{C}_2\text{H}_5)_2\text{H}^+$ ions have almost the same signal intensity and slope. In contrast, the Ge ion signals show a nonlinear dependence on the laser intensity.

At 266 nm, only Ge ion is generated even at a low laser intensity of 0.2 J/cm^2 , and its signal increases with the 2.5th order of laser intensity.

For TMG, when its molecular beam is focused with 355 nm, the Ge ion is mainly observed. Figure 3(A) shows the MPI mass spectrum of TMG at 8 mJ (2.1 kJ/cm^2) /pulse. The log value of signal vs. the log value of laser intensity (2-7 mJ/pulse) is plotted and its slope is found as 2.4 ± 0.1 . As the laser intensity at the molecular beam is decreased to 2.3 $\text{J}/\text{cm}^2 \cdot \text{pulse}$ by defocusing the laser beam, a strong $\text{Ge}(\text{CH}_3)_3^+$ ion peak appears, as shown in Figure 3(B). Figure 2(B) shows that the $\text{Ge}(\text{CH}_3)_3^+$ ion signal increases linearly with the laser intensity. At any intensity of 266 nm, MPI/TOF mass spectrum of TMG shows only Ge ion whose signal is dependent on the 2.5th order of the laser intensity.

We can summarize the results as follows: (1) Under high photon density of 355 nm and at 266 nm, the Ge ion is mainly produced from the multiphoton ionization/dissociation of TMG and TEG. The signal intensity depends on about the third order of laser intensity. (2) As the photon density of 355 nm decreases, the alkyl germanium ions are formed. For TEG, all ethyl germanium ionic species are produced, and for TMG the $\text{Ge}(\text{CH}_3)_3^+$ ion is mainly generated. The $\text{Ge}(\text{C}_2\text{H}_5)_2\text{H}^+$ ion is found for TEG. All alkyl germanium ion signals show a linear dependence on laser intensity.

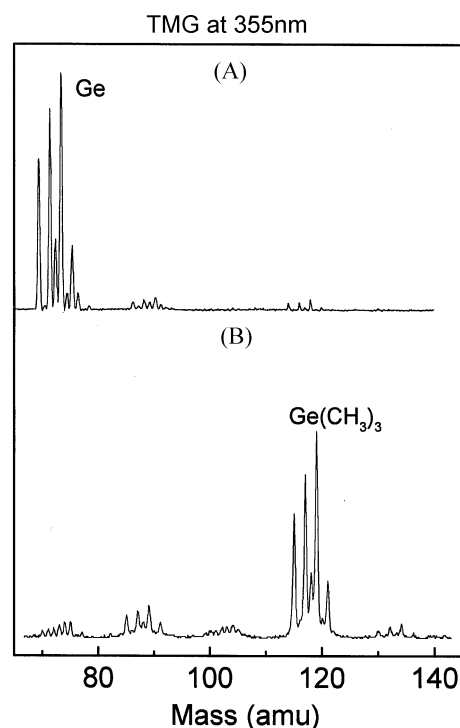
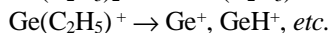
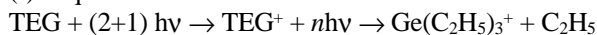


Figure 3. The MPI (355 nm)/TOF mass spectrum of TMG at (A) 2.1 kJ/cm^2 and (B) 2.3 J/cm^2 per pulse.

The experimental and theoretical bond energies of CH₃-Ge were reported to be in the range of 3.2-3.6 eV.⁶⁻⁸ The average bond energy Ge-C in the neutral molecule has been reported as 2.44 eV.⁹ The ionization energy of Ge is exactly 7.90 eV,¹⁰ and the ionization energy of TEG is estimated to be less than 9.8 eV.¹¹ Three photons of 266 nm (4.66 eV) and four photons of 355 nm (3.49 eV) are needed to dissociate four Ge-C bonds of TMG. Since the first absorption band of GeH₄ starts from 245 nm,¹² it is expected that for TMG and TEG, a 2 photon resonance excitation will occur by 355 nm and 266 nm, while 1 photon is necessary for the ionization.

The results suggest two independent channels involved in the photodissociation; one for the Ge ion production and another one for the alkyl germanium ion formation. The parent ion which is generated as a result of absorbing three photons, absorbs at least 4 photons of 355 nm to be dissociated into the Ge ion and alkyl fragments. If the parent ions undergo a unimolecular-type sequential dissociation, all kinds of alkyl germanium ion are produced. In the case of TEG, the Ge(C₂H₅)₂H⁺ ion can be produced via forming C₂H₄ (ethene) from the Ge(C₂H₅)₃⁺ ion, which provides an evidence for the unimolecular-type dissociation. If the slow step is the first Ge-alkyl bond dissociation of the parent ion, the formation of all the alkyl germanium ions would show a linear dependence on the laser intensity.¹³ On the other hand, when the dissociation takes place at once, only the Ge ion can be detected in mass spectrum. If the slow step is the (2+1)-photon absorption of the parent molecule, the Ge ion formation will be proportional to the third order of the laser intensity.¹³ At low intensity, the unimolecular-type sequential reaction can be dominant. But as the laser intensity increases, the parent ion absorbs more photons, and then the simultaneous dissociation becomes a dominant channel. At 266 nm, since even 3-photon energy is enough to lead the dissociation, the simultaneous dissociation can prevail under our experimental conditions. Thus, two channels for TEG are equated as follows:

(I) Sequential dissociation:



(II) Simultaneous dissociation:



The dissociation channels can also explain the experimental results of TMG. In the sequential dissociation, the dissociation of Ge(CH₃)₂⁺ into Ge(CH₃)₂⁺ probably needs more activation energy compared with Ge(C₂H₅)₃⁺ going to Ge(C₂H₅)₂H⁺ and C₂H₄. Thus the yield of the Ge(CH₃)₂⁺ ion is greatly reduced. If the dissociation energy of Ge-CH₃ of Ge(CH₃)₃ and of Ge-C₂H₅ of Ge(C₂H₅)₃ were measured or

calculated, the experimental results could be more clearly discussed.

Antman *et al.* measured the MPI/TOF mass spectrum at 355 nm for TEG, which mainly consisted of the parent and Ge ions.⁵ The ion signals display a linear dependence on the laser intensity. They also detected a non-mass selected REMPI signal of Ge neutral atom, showing third-order laser intensity dependence. They suggested two dissociation channels: one in which the Ge ion is formed from the parent ion by absorbing a number of photons, which is consistent with our finding, and another in which the excited parent molecule is dissociated into the Ge atom, which subsequently ionizes into Ge ion.

We report the MPI/TOF mass spectrum at 355 nm and 266 nm for Ge CVD precursors, TMG and TEG. We interpreted the experimental results by introducing two channels: one is the Ge ion formation directly by simultaneous dissociation and the other is the unimolecular-type sequential dissociation into the alkyl germanium ions. TEG can be sequentially dissociated via C₂H₄ or C₂H₆ formation. The simultaneous dissociation channel is dominant at 266 nm and at high laser intensity of 355 nm. We first compared the photoionization/dissociation mechanism of TEG and TMG by measuring the MPI/TOF mass spectrum.

Acknowledgment. This work was performed at Korea Research Institute of Standards and Science (KRISS) and supported by the Korea Science and Engineering Foundation (KOSEF 961-0305-052-2).

References

1. McClray, V. R.; Donnelly, V. M. In *Chemical Vapor Deposition: Principles and Applications*; Hichman, M. L., Jensen, K. F., Eds.; Academic Press: New York, 1993; pp 437-513.
2. Osmundsen, J. F.; Abele, C. C.; Eden, J. G. *J. Appl. Phys.* **1985**, *57*, 2921.
3. Fajgar, R.; Jakobukova, M.; Bastl, Z.; Pola, J. *Applied Surface Science* **1995**, *86*, 530.
4. Stanely, A. E. *J. Photochem. Photobio. A: Chemistry* **1996**, *99*, 1.
5. Antman, L.; Hilt, L.; Christophy, E.; BelBruno, J. J. *Chem. Phys. Lett.* **1994**, *221*, 294.
6. McMillen, D. F.; Golden, D. M. *Ann. Rev. Phys. Chem.* **1982**, *33*, 493.
7. Doncater, A. M.; Walsh, R. *J. Phys. Chem.* **1979**, *83*, 578.
8. Basch, H. *Inorg. Chim. Acta* **1996**, *252*, 265.
9. Lesbre, M.; Mazerolles, P.; Stage, J. *The Organic Compounds of Germanium*; Wiley: New York, 1971.
10. In *CRC Handbook of Chemistry and Physics* 76th ed.; Lide, D. R., Ed.; CRC Press: 1996.
11. de Ridder, J. J.; Dijkstra, G. *Rec. Trav. Chim.* **1967**, *86*, 737.
12. Itoh, U.; Toyoshima, Y.; Onuki, H.; Washida, N.; Ibuki, T. *J. Chem. Phys.* **1986**, *85*, 4867.
13. Bernstein, R. B. *J. Phys. Chem.* **1982**, *86*, 1178.